MIMO underwater acoustic communications over shallow water channel

Pierre-Jean BOUVET and Alain LOUSSERT
Underwater Acoustics Lab
ISEN Brest
C.S. 42807, 29228 BREST cedex 2 - FRANCE
Email: pierre-jean.bouvet@isen.fr

***Abstract*—Underwater acoustic channels are typically band-limited, reverberant and pose many obstacles to reliable high-speed digital communications. Recent progresses in digital modulation and channel decoding make current underwater acoustic modem fairly robust to time and frequency spreading of the channel. However the limited availability of underwater bandwidth prevents development of high data rate application. One approach for overcoming the limited bandwidth in the acoustic channel is the use of Multiple Input Multiple Output (MIMO) technology in which independent streams of information are transmitted from multiple transmit elements, simultaneously, all in the same bandwidth. In this paper we study the gain brought by MIMO techniques on underwater acoustic communications by considering the shallow water channel.**

I. Introduction

The past three decades have seen a growing interest in underwater acoustic communications (UAC) because of its applications in marine research, oceanography, marine commercial operations; the offshore oil industry and defense. However underwater acoustic channel characteristics such as fadings, extended multi-paths, bandwidth limitations or reverberation pose significant challenges to development of effective UAC systems [1] [2] [3]. On the other front, data rate required for UAC applications is continuously growing with the introduction of high quality images, real-time video as well as the deployment of autonomous underwater networks such as ad-hoc deployable sensor networks or autonomous fleets of cooperating unmanned undersea vehicles (UUV) [4].

First introduced in 90's in the field of radio communications, MIMO principle consists of transmitting digital data from N_t transmitters to N_r receivers within the same frequency band. Theoretical works and real-life experiments have demonstrated MIMO techniques to provide substantial data rate gain while keeping same robustness against fadings and transmission bandwidth unchanged [5] [6] [7] [8]. Recently, MIMO techniques have been applied to UAC systems. [9] [10]. Both simulation work and experimental results demonstrate large gain over conventional single input single output (SISO) transmission but these results are strongly linked to the chosen modulation scheme and receiver algorithm as well as underwater channel environment. The question of maximal MIMO gain on a information theoretic point is discussed in [11]. By using capacity analysis, authors of [11] showed that MIMO techniques are particularly well adapted to the so-called shallow water acoustic (SWA) channel.

Intention of our paper is to provide performance results of an ideal MIMO underwater system over the SWA channel by taking into account both underwater propagation and multi-path bandwidth limitation. For simplicity matters, performance results are performed in the frequency domain modeling an ideal multi-carrier transmission as proposed in [10].

Paper is organized as follows: section II describes the SWA channel model used for simulation. In section III we describe the theoretical MIMO communication system and especially algorithms used at transmit and receive side. Finally section IV provides system performance results and comparison with capacity bounds.

II. Shallow water channel model

Underwater acoustic propagation is characterized by limited bandwidth, extended multi-paths, refractive properties of the medium, severe fading, rapid time variation and large Doppler shifts. In the following, we will focus on the so-called shallow water channel corresponding to a water depth generally less than 100 m. Due to the proximity of surface and bottom interfaces, shallow water channel provides numerous multi-paths resulting in long delay spread and thus considered as the most challenging configuration for underwater acoustics communications.

A. Attenuation and noises

Underwater acoustic signals are affected by three attenuation mechanisms : spreading loss, absorption loss and reflection loss. Both spreading and absorption losses are frequency and range dependent and are usually represented by attenuation factor $A(l, f)$ defined as follows:

$$10 \log A(l, f) = k \cdot 10 \log l + l \cdot 10 \log \alpha(f) \qquad (1)$$

where k is the spreading factor describing the geometry of propagation (its commonly used values are $k = 2$ for spherical spreading, $k = 1$ for cylindrical spreading and $k = 1.5$ for the so-called practical spreading), l is the range of transmission,

f the frequency and $\alpha(f)$ the absorption coefficient provided empirically by Thorp's formula as a function of f in kHz [12] [13]:

$$10\log\alpha(f) = 0.11\frac{f^2}{1+f^2} + 44\frac{f^2}{4100+f^2} + 2.75{\cdot}10^{-4}f^2 + 0.003 \quad (2)$$

This formula is valid for $f > 400$ kHz, for lower frequencies, the formula becomes:

$$10\log\alpha(f) = 0.002 + 0.11\frac{f^2}{1+f^2} + 0.011f^2 \quad (3)$$

By hitting the sea-surface, sea-bottom or another under-sea object, the sound wave is partially or totally reflected depending on the wave frequency, the sound speed and the obstacle type. The reflection loss for path p is denoted Γ_p and will be described more in depth in the following sub-section. By taking into account all attenuation terms, the total path loss that occurs in a under-sea acoustic channel is equal to $\Gamma_p/\sqrt{A(l,f)}$.

On the frequency of interest of acoustic transmissions, under-sea communications are perturbed by an important ambient noise. Usually four sources are considered: turbulence, shipping, waves and thermal noise. These four noise components can be modeled by a colored Gaussian noise with following empirical power spectral density (p.s.d.) given in dB re μ Pa per Hz as a function of frequency in kHz [14] [15]:

$$10\log N_t(f) = 17 - 30\log f$$
$$10\log N_s(f) = 40 + 20(s-0.5) + 26\log f - 60\log(f+0.03)$$
$$10\log N_w(f) = 50 + 7.5w^{1/2} + 20\log f - 40\log(f+0.4)$$
$$10\log N_{th}(f) = -15 + 20\log f$$

where s is the shipping activity whose value ranges between 0 and 1 for low and high activity respectively whereas w is the wind speed expressed in m/s. The overall p.s.d. of the ambient noise is noted $N(f)$ and expressed as the sum of the four above mentioned noise components:

$$N(f) = N_t(f) + N_s(f) + N_w(f) + N_{th}(f) \quad (4)$$

This strong frequency dependency of the ambient noise is one of major factor considered when selecting frequency bands for underwater acoustics transmission.

B. Multi-paths propagation

Within a limited bandwidth, the acoustic signal is subject to multi-paths propagation through a channel whose characteristics vary with time and are highly dependent on the location of the transmitter and receiver. For simplicity reasons we will assume channel to be time invariant and will only consider multiple propagation paths from each source to receiver.

In order to predict the multi-path configuration, we use the isovelocity shallow water model developed in [16] where sound energy is conceptualized as propagating along straight lines with constant sound speed. The isovelocity assumption is justified as shallow water channel are usually well mixed and have relatively small increase in pressure over the depth of the water column. As illustrated in figure 1, the SWA channel is modeled as a wave guide consisting of an isovelocity layer (represented by the seawater) between two isovelocity half spaces: air and seabed.

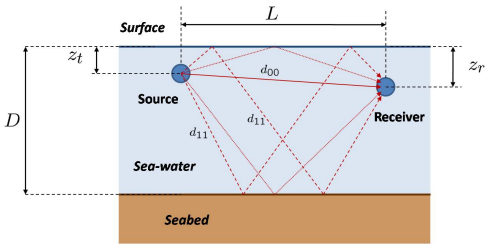

Fig. 1. Channel representation

Let L be the transmission range, D the water depth, z_t and respectively z_r be the depth of the transmitter and the receiver respectively. The distance traveled by the sound along various rays can be computed using geometrical approach. Let d_{sb} be the distance along an upward originating eigenrays with s surface reflections and b bottom reflections. The distance along a direct ray d_{00} is simply equal to:

$$d_{00} = \sqrt{L^2 + (z_t - z_r)^2} \quad (5)$$

In the general case, if $0 \leq s - b \leq 1$, the distance becomes [16]:

$$d_{sb} = \sqrt{L^2 + (2bD + z_t - (-1)^{s-b}z_r)^2} \quad (6)$$

Inversely, if $0 \leq b - s \leq 1$, we have:

$$d_{sb} = \sqrt{L^2 + (2bD - z_t + (-1)^{b-s}z_r)^2} \quad (7)$$

Attenuation coefficient due to reflection on surface denoted Γ^+ is relatively small in magnitude since the impedance mismatch between the seawater and air. If the sea is calm, reflection coefficient tends to perfect reflection value 1. If the sea surface is rough (due to waves), a small loss will be incurred for every surface interaction. This loss is modeled by a constant coefficient L_{SS}.

On the seabed boundary, the reflection coefficient Γ^- depends on the impedance variation from water to seabed. Such coefficient can be estimated using Rayleigh reflexion law as shown in [16]. Additional reflection losses due to rough or absorbing sea bottom are modeled by a constant coefficient L_{SB}.

Finally the total reflection loss for a path with s surface and b bottom reflections is equal to:

$$\Gamma_{sb} = \left(\Gamma^+ \cdot L_{SS}\right)^s \cdot \left(\Gamma^- \cdot L_{SB}\right)^b \quad (8)$$

The arrival time of each ray τ_{sb} is easily computed from the distance along the ray and sound speed:

$$\tau_{sb} = \frac{d_{sb}}{c} \quad (9)$$

By traveling from transmitter to receiver, each ray follows a path of length d_{sb} with arrival time τ_{sb} and an attenuation of $\Gamma_{sb}/\sqrt{A(d_{sb},f)}$. The SWA channel is modeled by taking account all possible paths and result in an Finite Impulse Response (FIR) filter with following transfer function [16]:

$$\begin{aligned} H(f) &= \frac{1}{\sqrt{A(d_{00},f)}} e^{-j2\pi f \tau_{00}} \\ &+ \sum_{s=1}^{+\infty} \sum_{b=s-1}^{s} \frac{\Gamma_{sb}}{\sqrt{A(d_{sb},f)}} e^{-j2\pi f \tau_{sb}} \\ &+ \sum_{b=1}^{+\infty} \sum_{s=b-1}^{b} \frac{\Gamma_{sb}}{\sqrt{A(d_{sb},f)}} e^{-j2\pi f \tau_{sb}} \end{aligned}$$

For practical computation, we'll assume that number of reflections on surface and sea-bottom is finite and equal to s_{max} and b_{max} respectively. Total number of paths is then equal to P with:

$$P = 1 + 2s_{max} + 2b_{max} \tag{10}$$

The channel transfer function can be rewritten as a closed-form expression:

$$H(f) = \sum_{p=0}^{P-1} \frac{\Gamma_p}{\sqrt{A(l_p,f)}} e^{-j2\pi f \tau_p} \tag{11}$$

where Γ_p , $A(d_p)$ and τ_p are the total reflection loss, the medium attenuation, and the arrival time of path p respectively.

C. MIMO model

A MIMO underwater channel connects N_t transmit hydrophones to N_r receive hydrophones. On the transmit and receive sides, each hydrophone pair has a vertical and constant separation of Δz_t and Δz_r respectively. The transmitter and receiver depths z_t and z_r correspond to the middle of each array as shown in figure 2. The MIMO array is placed in vertical direction in order to maximize delay spread difference between each sub-channels and thus minimize spatial correlation.

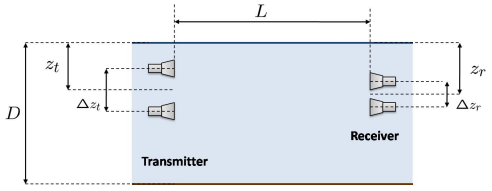

Fig. 2. MIMO SWA Channel representation

The MIMO channel is modeled by $N_t \times N_r$ sub-channels, where each sub-channel corresponds to the SWA channel model described in previous sub-section. As a result, the transfer function of sub-channel linking hydrophone $m \in [1, N_t]$ to hydrophone $n \in [1, N_r]$ denoted $H_{mn}(f)$ is simply derived from equation (11) as follows:

$$H_{mn}(f) = \sum_{p=0}^{P-1} \frac{\Gamma_p}{\sqrt{A(d_{p,mn},f)}} e^{-j2\pi f \tau_{p,mn}} \tag{12}$$

where $d_{p,mn}$ is the distance along the p-th path of sub-channel mn and $\tau_{p,mn} = d_{p,mn}/c$. The whole MIMO channel is represented by the following $N_r \times N_t$ channel matrix:

$$\mathbf{H}(f) = \begin{bmatrix} H_{11}(f) & \dots & H_{N_t 1}(f) \\ \vdots & \ddots & \vdots \\ H_{1N_r}(f) & \dots & H_{N_t N_r}(f) \end{bmatrix}_{N_r \times N_t} \tag{13}$$

III. System model

In this part we describe a theoretical MIMO UAC system model by using the MIMO SWA channel model presented in previous section. As illustrated in figure 3, the full system consists of a transmitter that converts the useful bits stream d into N_t signal streams sent simultaneously within the same band B to the MIMO SWA channel. At the receive side N_r output streams are demodulated and channel decoded leading to the estimated bit stream $\hat{d}$.

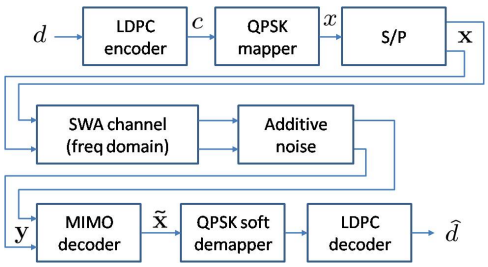

Fig. 3. MIMO 2×2 system simulator

A. Transmitter

Useful data d are first encoded using with a Linear Disperson Parity Check (LDPC) code of size $n = 256$ and $k = 128$, leading to an effective coding rate of $R_c = 1/2$ [17]. Encoded bits c are then converted into complex cells x using quadrature phase shift keying (QPSK) mapping, the modulation rate is thus $R_m = 2$. The stream of complex cells are finally divided into N_t independent streams leading to a spatial rate $R_s = N_t$. At a given sampling time, transmitted cells are modeled by vector $\mathbf{s} \in \mathbb{C}^{N_t \times 1}$.

The total transmit power P_s is assumed to be uniformly distributed over the bandwidth B and the N_t transmit hydrophones such as the power profile density (p.s.d.) of signal transmitted from hydrophone $m \in [1, N_t]$ can be expressed as:

$$S(f) = \frac{P_S}{B \cdot N_t} \quad , \forall f \in \left[f_0 - \tfrac{B}{2}, f_0 + \tfrac{B}{2} \right] \tag{14}$$

where f_0 is center carrier frequency around which the signal is transmitted.

B. Channel

The MIMO SWA channel takes as input N_t streams and provides N_r output streams. In order to simplify encoding and decoding algorithms, we consider the MIMO SWA channel in the frequency domain representing an OFDM like system as

described in [10]. The received vector $\mathbf{y} \in \mathbb{C}^{N_r \times 1}$ can thus be expressed as follows:

$$\mathbf{r} = \mathbf{H} \cdot \mathbf{s} + \mathbf{n} \tag{15}$$

where $\mathbf{H}$ is a frequency realization of the MIMO matrix introduced in (13) and $\mathbf{n} \in \mathbb{C}^{N_t \times 1}$ the additive noise vector obtained by filtering a complex white gaussian noise process leading to the underwater acoustic noise d.s.p. described in (4). The total noise power is equal to:

$$P_N = \int_{f_0 - B/2}^{f_0 + B/2} N(f) df \tag{16}$$

At receive side, the total power receive from hydrophone $n \in [1, N_r]$ is equal to:

$$P_{Rn} = \int_{f_0 - B/2}^{f_0 + B/2} R_n(f) df \tag{17}$$

where R_n is received signal p.s.d. viewed by hydrophone n:

$$R_n(f) = \sum_{m=1}^{N_t} |\mathbf{H}_{mn}(f)|^2 S(f) \tag{18}$$

As a result the signal-to-noise ratio viewed at receive hydrophone $n \in [1, N_r]$ can be expressed as:

$$SNR_n = \frac{P_{Rn}}{P_N} \tag{19}$$

C. Receiver

At receive side, vector $\mathbf{r}$ is first processed by the MIMO decoder which uses the estimation of channel matrix $\mathbf{H}$ (assumed to be perfect) in order to produce the equalized vector $\tilde{\mathbf{s}}$ with the following algorithm:

$$\tilde{\mathbf{s}} = \mathbf{W}^H \mathbf{r} \tag{20}$$

where the equalization matrix $\mathbf{W}^H$ is the solution of the linear filter optimization under the Zero-Forcing criterion [18]:

$$\mathbf{W}^H = \left(\mathbf{H}^H \mathbf{H}\right)^{-1} \mathbf{H}^H \tag{21}$$

where $(.)^H$ stands for transpose conjugate operand.

Equalized cells are then converted into log-likelihood ratio (LLR) using a QPSK soft demapper. The LLR of bit $i \in [1, 2]$ belonging to cells $m \in [1, N_t]$ is computed as [18]:

$$LLR(i, m) = \frac{4}{\gamma_m^2} \left[\min_{s \in \mathcal{A}_0^i} \left| \tilde{s}_m - s \right|^2 - \min_{s \in \mathcal{A}_1^i} \left| \tilde{s}_m - s \right|^2 \right] \tag{22}$$

where A_b^i denotes the subset of the QPSK constellation for which the i-th bit is equal to b and γ_m^2 is (m, m) entry of matrix $\sigma^2 \cdot \mathbf{W}^H \mathbf{W}$ with σ^2 the noise power observed around the frequency f over the frequency resolution Δf.

$$\sigma^2 = \int_{f - \Delta f}^{f + \Delta f} N(f) df \tag{23}$$

The soft LLR information on each bit is finally passed to the LDPC channel decoder that produces decoded bits using a classical min-sum algorithm [19].

TABLE I
SIMULATION PARAMETERS

Letter	Name	Default value
f_0	Carrier frequency	32 kHz
B	Signal Bandwidth	12 kHz
F_s	Sampling frequency	500 kHz
Δf	frequency resolution	7.6 Hz
L	Range	1500 m
D	Water depth	20 m
N_t	Number on transmit transducers	2
N_r	Number on receive transducers	2
z_t	Transmit array depth	9 m
Δz_t	Vertical separation of transmit array	0.6 m
z_r	Receive array depth	9 m
Δz_r	Vertical separation of receive array	0.6 m
k	Spreading factor	1.5
c	Sound speed in water	1500 m/s
ρ	Water density	1023 kg/m^3
c_1	Sound speed in sea-bottom	1650 m/s
ρ_1	Sea-bottom density	1500 kg/m^3
L_{SS}	Absorption loss at sea-surface	-0.5 dB
L_{SB}	Absorption loss at sea-bottom	-3 dB

TABLE II
SPECTRAL EFFICIENCIES

System model	LDPC rate R_c	Mod. rate R_m	Spatial Rate R_s	Spec. Eff. ν [bps/Hz]
SISO	1/2	2	1	1
MIMO 2×2	1/2	2	2	2
MIMO 4×4	1/2	2	4	4

IV. NUMERICAL RESULTS

A. Simulation set-up

Channel parameters chosen for simulation works are summarized in Table I. These parameters are derived from MIMO experiments made in [10]. The SWA channel is numerically evaluated with a frequency resolution equals to $\Delta f = 7.6$ Hz. By assuming no bandwidth loss within the transmission signal, spectral efficiency ν is computed as:

$$\nu = R_c \cdot R_m \cdot R_s \quad [\text{bits/s/Hz}] \tag{24}$$

Values of ν for several hydrophone configurations including single input single output (SISO) system are given in table II.

B. BER results

Figure 4 provides bit error rate (BER) results obtained for both SISO and MIMO system models as a function of SNR. As a reference the performance of additive white Gaussian noise (AWGN) transmission is plotted in the same figure. All system performances are at minimum of 5 dB from the AWGN curves confirming the intrinsic difficulty of SWA channel. For a target BER of 10^{-4}, one can notice that the two MIMO systems exhibit a increasing SNR penalty with respect to SISO

SWA curve as the hydrophone number increases. This can be easily explained by the fact that MIMO architecture provides co-antenna interference terms contributing as additional noise sources. However this SNR loss is converted into data-rate gain since the 2×2 and 4×4 systems carry respectively 2 times and 4 times more bits per second per Hertz than the SISO configuration.

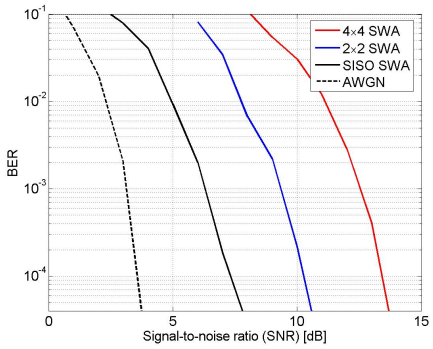

Fig. 4. BER results of MIMO 2×2 and SISO SWA system model as function of SNR.

C. Capacity comparisons

The channel capacity represents the maximum amount of information that can be reliably transmitted over a communications channel. In case of deterministic MIMO, E. Telatar provided the general expression of the MIMO capacity in [5]. In [11], the authors derived the capacity formula for a MIMO SWA channel:

$$C(f) = \log_2 \det \left(\mathbf{I}_{N_t} + \frac{S(f)}{N_t \cdot N(f)} \mathbf{H}(f) \mathbf{H}(f)^H \right) \qquad (25)$$

The total channel capacity is obtained by integrating $C(f)$ over the transmit bandwidth B:

$$C = \int_{f_0 - B/2}^{f_0 + B/2} C(f) df \quad [\text{bits/s/Hz}] \qquad (26)$$

Figure 5 provides numerical evaluation of capacities over the above considered SWA channels. Capacity is drawn for the SISO, MIMO 2×2 and MIMO 4×4 configurations as a function of SNR. We also add on the same plot, simulation results obtained in the previous sub-section for the same channel configuration with a target BER assumed to be 10^{-4} and the associated spectral efficiencies (see table II). One can see that simulated system results are far away from the capacity. There are two reasons explaining this result: on the one hand MIMO decoder is very simple but quite sub-optimal and could be substantially improved: maximum a posteriori (MAP) decoder or iterative based approach would dramatically improve BER for a same SNR [18]. On the other hand, capacity computation assumes Gaussian distribution of the complex cells which is not our case since QPSK mapping is used. However despite the loss in SNR, performance results demonstrate that MIMO provide a substantial capacity gain since 4×4 system outperforms SISO capacity which corresponds to the best achievable performance of a SISO system.

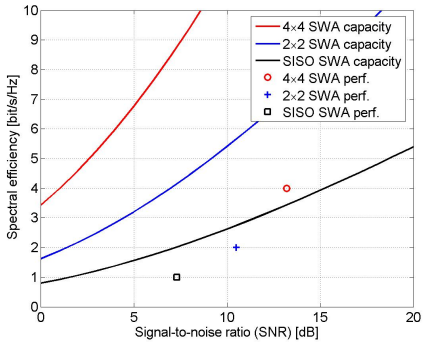

Fig. 5. Capacity results of MIMO 2×2 and SISO SWA system model as function of SNR.

V. Conclusions

The primary aim of this study was to verify by simulation the capacity gain brought by MIMO technology for underwater acoustic communication. By using frequency response of a shallow water acoustic channel model, the paper provides a theoretical transmission chain modeling an ideal MIMO underwater acoustic communication. Monte-carlo simulations performed for different MIMO configurations as well as comparisons with capacity results demonstrate that MIMO approach provides data-rate gain but at the price of a SNR loss. However on a practical point of view, the SNR penalty brought by MIMO decoding would not be a limiting factor since synchronization and channel estimation algorithms usually requires SNRs greater than 15 dB. Furthermore the use of more efficient MIMO decoder would reduce this SNR penalty.

References

[1] R. F. W. Coates, *Underwater Acoustic Systems*. Wiley, 1989.

[2] M. Stojanovic, "Recent advances in high-speed underwater acoustic communications," *IEEE J. Ocean. Eng.*, vol. 121, no. 2, pp. 125–136, Apr. 1996.

[3] R. S. H. Istepanian and M. Stojanovic, *Underwater acoustic digital signal processing and communication systems*. Kluwer Academic Pub., 2002.

[4] I. F. Akyildiz, D. Pompili, and T. Melodia, "Underwater acoustic sensor networks: research challenges," *Ad Hoc Network Jorunal*, vol. 3, no. 3, pp. 257–279, 2005.

[5] E. Telatar, "Capacity of multiantenna gaussian channel," *Bell Labs. Tech. Memo.*, Jun. 1995.

[6] G. J. Foschini, "Layered space-time architecture for wireless communication in a fading environment when using multielement antennas," *Bell Syst. Tech. Journal*, vol. 1, pp. 41–59, Oct. 1996.

[7] D. Gesbert, M. Shafi, D. Shiu, and P. Smith, "From theory to practice: An overview of space-time coded mimo wireless systems," *IEEE J. Sel. Areas Commun.*, Apr. 2003.

[8] A. Paulraj, A. D. Gore, R. U. Nabar, and H. Boelcskei, "An overview of MIMO communications: A key to gigabit wireless," *Proceedings of the IEEE*, vol. 92, no. 2, pp. 198–218, Feb. 2004.

[9] D. B. Kilfoyle, J. C. Preisig, and A. B. Baggeroer, "Spatial modulation experiments in the underwater acoustic channel," *IEEE J. Ocean. Eng.*, vol. 30, no. 2, pp. 406–415, Apr. 2005.

[10] B. Li, J. Huang, S. Zhou, K. Ball, M. Stojanovic, L. Freitag, and P. Willett, "MIMO-OFDM for high rate underwater acoustic communications," *IEEE J. Ocean. Eng.*, vol. 34, no. 4, pp. 634–644, 2009.
[11] P.-J. Bouvet and A. Loussert, "Capacity analysis of underwater acoustic mimo communications," in *Proceedings of OCEANS'10*, 2010.
[12] W. H. Thorp, "Analytic description of the low frequency attenuation coefficient," *Journal of the Acoustical Society of America*, vol. 33, pp. 334–340, 1961.
[13] F. H. Fisher and V. P. Simons, "Sound absorption in seawater," *Journal of the Acoustical Society of America*, vol. 62, pp. 558–564, 1977.
[14] R. J. Urick, *Ambient Noise in the Sea*. Peninsula Pub, 1986.
[15] M. Stojanovic, "On the relationship between capacity and distance in an underwater acoustic communication channell," *ACM SIGMOBILE Mobile comput. and Comm. Review (M2CR)*, vol. 11, pp. 34–43, Oct. 2007.
[16] M. A. Chitre, "A high-frequency warm shallow water acoustic communications channel model and measurements," *Journal of the Acoustical Society of America*, vol. 5, no. 122, pp. 2580–2586, 2007.
[17] D. J. MacKay and R. M. Neal, "Near shannon limit performance of low density parity check codes," *Electronics Letters*, vol. 32, pp. 1645–1646, 1996.
[18] P.-J. Bouvet, M. Helard, and V. L. Nir, "Simple iterative receivers for MIMO LP-OFDM systems," *Annals of telecomm.*, vol. 61, no. 5-6, 2006.
[19] A. B. F. Zarkeshvari, "On implementation of min-sum algorithm for decoding low-density parity-check (LDPC) codes," in *Proceedings of Globecom'02.*, 2002.